Lung Ventilation/Perfusion SPECT in the Artificially Embolized Pig

Marika Bajc, MD, PhD[1]; Ulrika Bitzén, MD[1]; Berit Olsson[1]; Valéria Perez de Sá, MD[2]; John Palmer, PhD[3]; and Björn Jonson, MD, PhD[1]

[1]Department of Clinical Physiology, Lund University Hospital, Lund, Sweden; [2]Department of Anesthesiology, Lund University Hospital, Lund, Sweden; and [3]Department of Radiation Physics, Lund University Hospital, Lund, Sweden

Planar lung scintigraphy is a standard method used for the diagnosis of lung embolism, but it is hampered by the high incidence of nondiagnostic tests. Ventilation/perfusion SPECT may possibly improve this situation. The objective of this study was to compare planar lung scintigraphy with ventilation/perfusion SPECT using pigs with artificially engendered lung emboli labeled with ^{201}Tl. **Methods:** Sixteen anesthetized pigs were each injected with zero to 4 latex emboli. Cylindric emboli were used in the first 7 pigs and flat 3-tailed emboli were used in the remaining 9 pigs. The pigs spontaneously inhaled 30 MBq ^{99m}Tc-diethylenetriaminepentaacetic acid aerosol for ventilation scintigraphy. Planar scintigraphy and SPECT were performed using a double-head gamma camera in ^{99m}Tc and ^{201}Tl windows. Immediately thereafter, 100 MBq ^{99m}Tc-labeled macroaggregated albumin were injected intravenously followed by SPECT and, finally, planar scintigraphy. The ventilation background was subtracted from the perfusion tomograms for calculation of a normalized ventilation/perfusion (V/P) quotient image set. **Results:** The cylindric emboli caused artifacts in the ventilation images; therefore, these were excluded from the final analysis. However, for the planar perfusion images of these pigs, sensitivity and specificity were 71% and 91%, respectively, whereas SPECT yielded 100% for both. For the 3-tailed emboli and ventilation/perfusion images, the sensitivity and specificity were 64% and 79%, respectively, for the planar modality, whereas SPECT yielded values of 91% and 87%, respectively. **Conclusion:** V/P SPECT may improve the diagnostic power of lung scintigraphy.

Key Words: lungs; SPECT; embolism; ventilation; perfusion; pig

J Nucl Med 2002; 43:640–647

Planar lung scintigraphy is the most frequently used method for the diagnosis of lung embolism (*1*) because of its noninvasive character, ease of application, low cost, low radiation burden, and high sensitivity (*2*). On the basis of the Prospective Investigation of Pulmonary Embolism Diagnosis (PIOPED), and modified PIOPED interpretative strategies, the incidence of nondiagnostic findings has been high, which has resulted in a controversy concerning the value of scintigraphy (*3–5*). Indeed, the lack of specificity is an important problem when using only perfusion scintigraphy for the delineation of perfusion defects on planar images. Such shortcomings have stimulated the development of spiral CT, which now challenges the role of lung scintigraphy. It has been suggested that spiral CT may even replace, rather than complement, scintigraphy (*6*). However, spiral CT is less than perfect; it is known to have limited performance in terms of nondiagnostic CT scans (estimated at approximately 15%), causing false-positive and false-negative results (*7*). A problem in evaluating noninvasive techniques in general is that even invasive angiography is imperfect, although it has been used as the gold standard for the diagnoses of lung emboli. Baile et al. (*8*), using a methacrylate cast of the porcine pulmonary vessels as the independent gold standard, showed that angiography has a sensitivity of only 87% for emboli that are equivalent in size (3.8 and 4.2 mm) to human subsegmental pulmonary vessels. Corbus et al. (*9*), Magnussen et al. (*10*), and Wenger et al. (*11*) suggest that SPECT improves the specificity of scintigraphy and decreases significantly the number of intermediate probability results. Palmer et al. (*12*) have shown that ventilation/perfusion (V/P) SPECT is clinically feasible, with a short examination time, a low cost, and a low radiation dose. It is also claimed that it yields improved detectability and characterization of perfusion defects in patients studied with respect to lung embolism. On this basis it is suggested that future comparisons should be made between spiral CT and scintigraphy taking into account the latest developments in each technique. At this time, it is judged that scintigraphic techniques need to be refined to match recent developments in CT.

The aim of this study was to compare tomographic and planar techniques used for perfusion and ventilation studies with respect to the diagnostic power for low-degree embolism. Small emboli, labeled with ^{201}Tl, were administered to pigs, which constitutes an independent gold standard for identification of embolized lung areas.

Received Apr. 4, 2001; revision accepted Sep. 25, 2001.

For correspondence or reprints contact: Marika Bajc, MD, PhD, Department of Clinical Physiology, Lund University Hospital, S-221 85 Lund, Sweden.

E-mail: marika.bajc@klinfys.lu.se

MATERIALS AND METHODS

The local ethics board of animal research approved the experimental protocol for these studies. Sixteen pigs (weight, approximately 30 kg) were used. The animals were premedicated with an intramuscular injection of azaperon (Stresnil; Jansen, Beerse, Belgium), 6 mg/kg. To diminish salivation, 0.5 mg atropine (Atropin NM; Pharma AB, Stockholm, Sweden) was given intravenously 30 min before administration of anesthesia. This was induced by injection of 300 mg ketamine hydrochloride (Ketalar; Parke-Davis, Warner-Lambert Nordic, Solna, Sweden) into an ear vein before orotracheal intubation. Anesthesia was maintained by a continuous infusion of ketamine hydrochloride, 17 mg/kg/h, and midazolam (Dormicum; Hoffmann-La Roche AG, Basel, Switzerland), 1.7 mg/kg/h. The animals breathed spontaneously throughout the study period. The heart rate and intraarterial blood pressure were monitored continuously. An introducer sheath (Intradyn arterial F12; Braun Melsungen AG, Melsungen, Germany) placed in the superior vena cava by direct puncture above the sternal notch was used to inject emboli. To avoid the buildup of thrombotic material on the emboli, 2,500 units heparin (Heparin Leo; Leo Pharma AB, Malmö, Sweden) were administered intravenously.

Two types of emboli were manufactured; the first were cylindric latex balloons 15 mm long with diameters of 2.2, 2.8, 3.2, and 3.7 mm filled with 0.1–0.5 MBq ^{201}Tl and sealed with silicon. The second type was fabricated using 0.4-mm-thick latex material in which ^{201}Tl was mixed in the suspension constituting the raw material. Three strips of this material, 2 to 2.5 mm wide and 29, 31, and 35 mm long, were then glued together at 1 end to form flat emboli with 3 tails; the density of this arrangement was similar to that of blood thrombi. The size was chosen so that the emboli would lodge in vessels comparable to human subsegmental arteries. The low activity of ^{201}Tl and its low-energy spectrum imply that ^{201}Tl does not influence images obtained in the ^{99m}Tc window.

SPECT Acquisition Parameters

A large-field-of-view dual-head gamma camera was used (DST-Xli; Sopha Medical Vision International, Buc, France). The inhaled activity for ventilation scintigraphy was 30 MBq ^{99m}Tc-diethylenetriaminepentaacetic acid (DTPA) (TechneScan DTPA; Mallinckrodt Medical BV, Petten, The Netherlands). The pigs inhaled the aerosol from a pressurized-air–driven nebulizer as described (*13*). Inhalation was terminated when the counting rate from the gamma camera indicated that 30 MBq ^{99m}Tc-DTPA had been deposited in the lungs. Planar imaging and SPECT imaging were then performed. At the completion, 100 MBq ^{99m}Tc-labeled macroaggregated albumin (MAA) (TechneScan LyoMAA; Mallinckrodt Medical BV) were injected intravenously. The perfusion study followed immediately. For the first 7 pigs, injected with cylindric emboli, a high-resolution collimator and a 128 × 128 matrix were used for acquisition, which yields higher resolution when clinical restrictions such as acquisition time or activity dose is not considered (*12*). For the remaining 9 pigs, our standard clinical acquisition parameters were used: a low-energy all-purpose collimator and a 64 × 64 matrix with 128 projections over 360°. To accommodate the smaller overall lung size of the pigs, the pixel size was changed from 6.8 to 5.6 mm. An earlier study showed that the entire procedure could be completed within 30 min (*12*). For optimal results, the counting rate at perfusion should be 4 times that of the ventilation study, while using one third of the available acquisition time. Sixty-four steps, each of 10-s duration, were used for the ventilation study, and of 5-s duration for the perfusion study. ^{99m}Tc-DTPA clearance was calculated from the initial and final SPECT projections and was then used for correction of the ventilation projection set before reconstruction. Iterative reconstruction was performed for ventilation and perfusion using ordered-subsets expectation maximization with 8 subsets and 2 iterations. The ventilation background was subtracted from the perfusion tomograms, and a systematically normalized V/P image set was calculated as described (*12*).

Experimental Protocol

The first 7 pigs, of which 5 were embolized, were used for the initial tests of the model for lung embolization. Zero to 4 cylindric emboli were injected in each pig. In the remaining 9 pigs, of which 7 were embolized, 3-tailed latex emboli were used. Zero to 4 emboli were randomized for each pig. After injection of each embolus, a planar image in the ^{201}Tl window was obtained to identify the site of embolus lodging in the lung. One hour after embolization, inhalation of ^{99m}Tc-DTPA aerosol was followed by acquisition of planar images in 4 projections. SPECT was performed thereafter, first in the ^{99}Tc window and then in the dual-mode, ^{99}Tc and ^{201}Tl, window. Without moving the pig, perfusion SPECT was performed after an intravenous injection of ^{99m}Tc-MAA. Planar perfusion images followed SPECT. The pig was killed with concentrated potassium chloride (Addex-Kaliumklorid; Fresenius Kabi, Uppsala, Sweden) injected intravenously.

Interpretation Criteria

All images were interpreted from a computer display, which allowed adjustment of thresholds and colors. For the group of 7 pigs, of which 5 were embolized with cylindric emboli, 2 physicians who were unaware of the number of emboli injected reviewed, in 2 separate sessions, all planar and tomographic images. The order of pigs was randomized in each session. Increased activity adjacent to the emboli was observed on the ventilation images of some pigs injected with cylindric emboli. Because this could affect the interpretation of perfusion images, these ventilation images were not shown to the interpreter. Each perfusion defect considered to reflect lung embolization, regardless of size, was described.

In the second group of 9 pigs, 7 were embolized with 3-tailed emboli and 2 were not embolized. For this group, 3 physicians reviewed all images recorded in the ^{99m}Tc window in 2 sessions as above, but using ventilation and perfusion images. On sagittal, coronal, and transversal slices the reviewer first identified perfusion defects within well-ventilated areas, which were considered to reflect lung emboli, regardless of size. These were noted as perfusion defects. For the same pig, V/P quotient slices were then displayed together with corresponding ventilation and perfusion slices. In addition, the lung volume was also displayed in a 3-dimensional rotating synchronized display over ventilation, perfusion, and V/P quotient. Any change in the interpretation based on this additional information was noted.

A fourth interpreter studied images taken in the ^{201}Tl window. First, on planar images, this reader identified emboli after each injection. Emboli that lodged at the same place were identified by an approximately 2-fold increased local activity. Later, on SPECT images, the precise localizations of emboli were identified. Perfusion defects peripheral to the site of embolus lodging were considered to represent true-positive findings; the others were classified as false-positive findings. When a perfusion defect was not identified, despite the presence of an embolus, this was deemed a false-negative finding. A lung without embolus, in which no per-

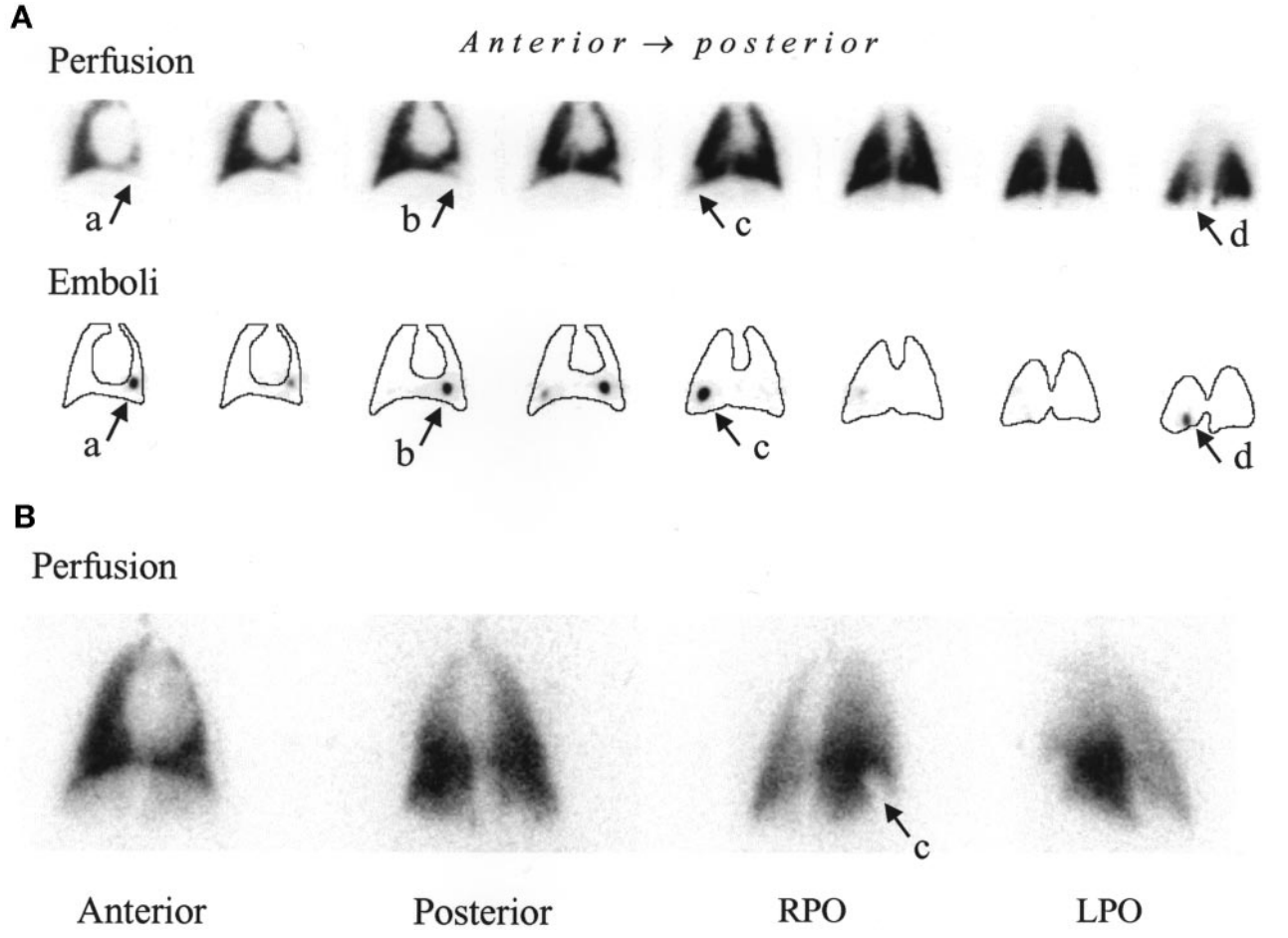

FIGURE 1. (A) Tomography. Consecutive perfusion coronal slices and simultaneously acquired matching ^{201}Tl images of emboli. In left lung, 2 emboli (a and b) caused 1 large perfusion defect. In right lung, 2 emboli caused 2 perfusion defects (c and d). (B) Planar images of same pig as in A. Both readers observed only 1 perfusion defect (c). RPO = right posterior oblique; LPO = left posterior oblique.

fusion defect was identified, was classified as a true-negative finding.

RESULTS

All injected emboli, 19 cylindric and sixteen 3-tailed, were identified within the lungs using the ^{201}Tl window. Of the total of 35 emboli, 24 were impacted in the right lung, often very peripherally in the lower lobe. Some emboli lodged close to each other, although they were injected separately.

Of the 19 cylindric emboli, 2 lodged together in each lung of 1 pig and 3 lodged together in another pig. Each of these doublets or triplets caused a single perfusion defect. On 1 occasion, 2 emboli created 1 large perfusion defect, although they were lodged at some distance from each other (Fig. 1). Each of the remaining 10 emboli was the cause of a single perfusion defect. Accordingly, the 19 cylindric emboli caused 14 perfusion defects, which were localized in 9 lungs (Table 1). On the planar images, both readers identified 10 true-positive perfusion defects (Table 2): Among the 4 false-negative results, both readers agreed in 2 cases. For the 2 readers, the average sensitivity and specificity were 71% and 91%, respectively. For the tomographic images, both readers observed 14 true-positive perfusion defects and zero false-positive perfusion defects; sensitivity and specificity were 100%.

Among sixteen 3-tailed emboli, 2 emboli lodged together well within the observed borders of the lung on 2 occasions and caused a single perfusion defect (Fig. 2). Another 2 emboli lodged together on the extreme lung periphery, at a site distal to which neither ventilation defect nor perfusion defect was observed (Fig. 3). On 3 occasions, 2 distinct

TABLE 1
Number of Emboli and Perfusion Defects Caused by Emboli

Type of emboli	Nonembolized lung	Embolized lung	No. of emboli	No. of perfusion defects
Cylindric	5	9	19	14
3-Tailed	10	8	16	15

TABLE 2
Positive and Negative Findings on Planar and SPECT Perfusion Images of Pigs Embolized with Cylindric Emboli

	Planar images: perfusion						Tomographic images: perfusion					
Reader	True-positive	False-positive	True-negative	False-negative	Sensitivity (%)	Specificity (%)	True-positive	False-positive	True-negative	False-negative	Sensitivity (%)	Specificity (%)
1	10	1	5	4	71	83	14	0	5	0	100	100
2	10	0	5	4	71	100	14	0	5	0	100	100

perfusion defects were observed peripherally to a single embolus. On all of these occasions, all 3 observers identified the perfusion defects on tomographic images. For a 3-tailed embolus lodged in a bifurcation, it is possible that 2 perfusion defects are produced. On these occasions, the interpretation was that 2 perfusion defects were caused by a single embolus. Thus, at 15 locations, perfusion defects caused by emboli were present (Table 1). With the planar modality, sensitivity among the 3 readers was on average 64% and specificity was 79%. On tomographic images, sensitivity was on average 91% and specificity was 87% (Table 3). With both modalities, all readers observed 1 perfusion defect in 1 and the same embolized pig but in the nonembolized lung (Fig. 4).

In most instances the delineation of perfusion defects was quite obvious on the tomographic images of ventilation and perfusion (Fig. 2). However, all 3 readers observed that the addition of the V/P quotient facilitated the interpretation. The joint 3-dimensional cine presentation of ventilation, perfusion, and V/P quotient offered further support. Because the pigs were young and apparently healthy, ventilation was in general uniform. Ventilation images allowed delineation of the lung border, which was considered essential for interpretation of the small peripheral perfusion defects that were caused, particularly, by the 3-tailed emboli. In a single pig, the ventilation was distributed unevenly (Fig. 2). In 4 of 9 pigs, an increased deposition of aerosol around the heart was observed (Fig. 2). This pattern was not regarded as a sign of embolization because it does not follow pig lung-segment orientation.

DISCUSSION

The animal model of lung emboli prelabeled with ^{201}Tl allows precise localization of the emboli and, thereby, adequate evaluation of perfusion defects on planar and SPECT images. Consequently, problems caused by the imperfection of other modalities used for comparison, such as angiography or spiral CT (*8*), were avoided. The gold standard offered by the labeled emboli was a prerequisite behind the conclusive evidence that SPECT is superior to planar imaging in the detection of small perfusion defects.

Although practical issues required the use of pigs smaller than adult man, they were of adequate size for our purposes (*8*). A problem with pigs is that the main pulmonary arterial trunk has a straight course with lateral branches of varying size rather than the dichotomic divisions in humans (*14*). This probably contributed to peripheral lodging of emboli, which was extreme in some instances. Another difficulty with pigs was the increased deposition of aerosol around the heart (Fig. 2). This was not observed in 15 patients who were studied with the same technique (*12*). A tentative explanation is that large heart movements in pigs increase alveolar retention of aerosol particles. All of these issues, combined with the readers' lack of experience in dealing with lung morphology and pig vessels, implied some difficulties in the interpretation. The good health of the animals balanced these difficulties.

The size of the cylindric emboli was chosen to be equivalent to that of subsegmental vessels in humans and was comparable with the sizes used by Baile et al. (*8*). These emboli caused quite distinct perfusion defects but also increased deposition of aerosol close to the embolus, probably reflecting turbulence induced by deformation of the adjacent bronchus. The distinct perfusion defects may indicate that the shape of these emboli led to a complete plugging of the artery, which together with the particularly high resolution of the images in the first series of pigs gave 100% sensitivity and specificity on SPECT.

To better mimic natural emboli, the 3-tailed flat emboli were developed. These emboli did not cause a local deposition of aerosol and probably allowed some blood to seep past them. When the series of pigs with 3-tailed emboli was studied, the tomographic method had been adapted to clinical requirements. Accordingly, recommended isotope doses and a total acquisition time of 20 min, including ventilation and perfusion, were applied. Also, a general-purpose collimator and a matrix size of 64 × 64 were judged appropriate, although this resulted in a slightly lower resolution (*12*).

The series of pigs with cylindric emboli showed a superiority of SPECT over planar imaging. The advantage of SPECT was verified in the pathophysiologically and clinically more realistic situation modeled in the second series of pigs. The main reason for the lower performance of the planar modality is probably the inferior contrast between lesions and normal areas resulting from superposition of surrounding activity onto lesions. Planar images do not provide an accurate comparison between ventilation and perfusion, which is especially relevant for detection of small defects. In the series with the 3-tailed emboli, the ventilation images and, particularly, the V/P quotient images were considered important for the interpretation. Without ventilation and the V/P quotient images, delineation of the lung

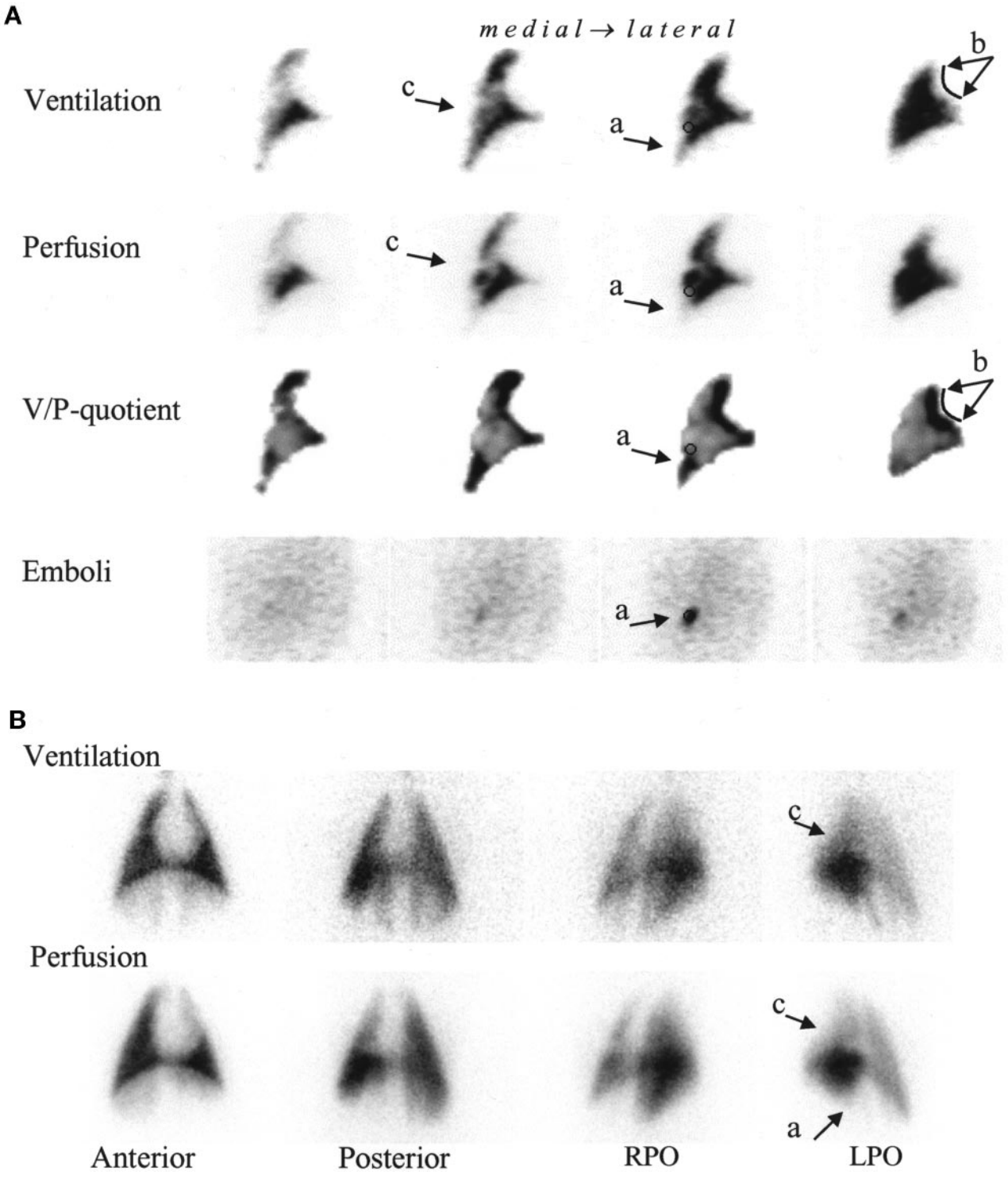

FIGURE 2. (A) Tomography. Sagittal slices of left lung: 2 emboli lodged at same location, causing single perfusion defect (a). On ventilation and V/P quotient images, increased deposition of aerosol is observed around heart (b). Diminished ventilation and perfusion are observed in 1 region (c), leaving V/P quotient essentially unchanged. (B) Planar images of same pig as in A; same changes as shown in A are observed but not as clearly. RPO = right posterior oblique; LPO = left posterior oblique.

would not be evident and perfusion defects resulting from small peripheral emboli would be missed. Differentiation between embolization leading only to perfusion defects (mismatch) and other pathology leading to combined defects of ventilation and perfusion (match) is a commonly observed rationale of ventilation scintigraphy. In this series of generally healthy pigs, the latter feature was of value only in some instances.

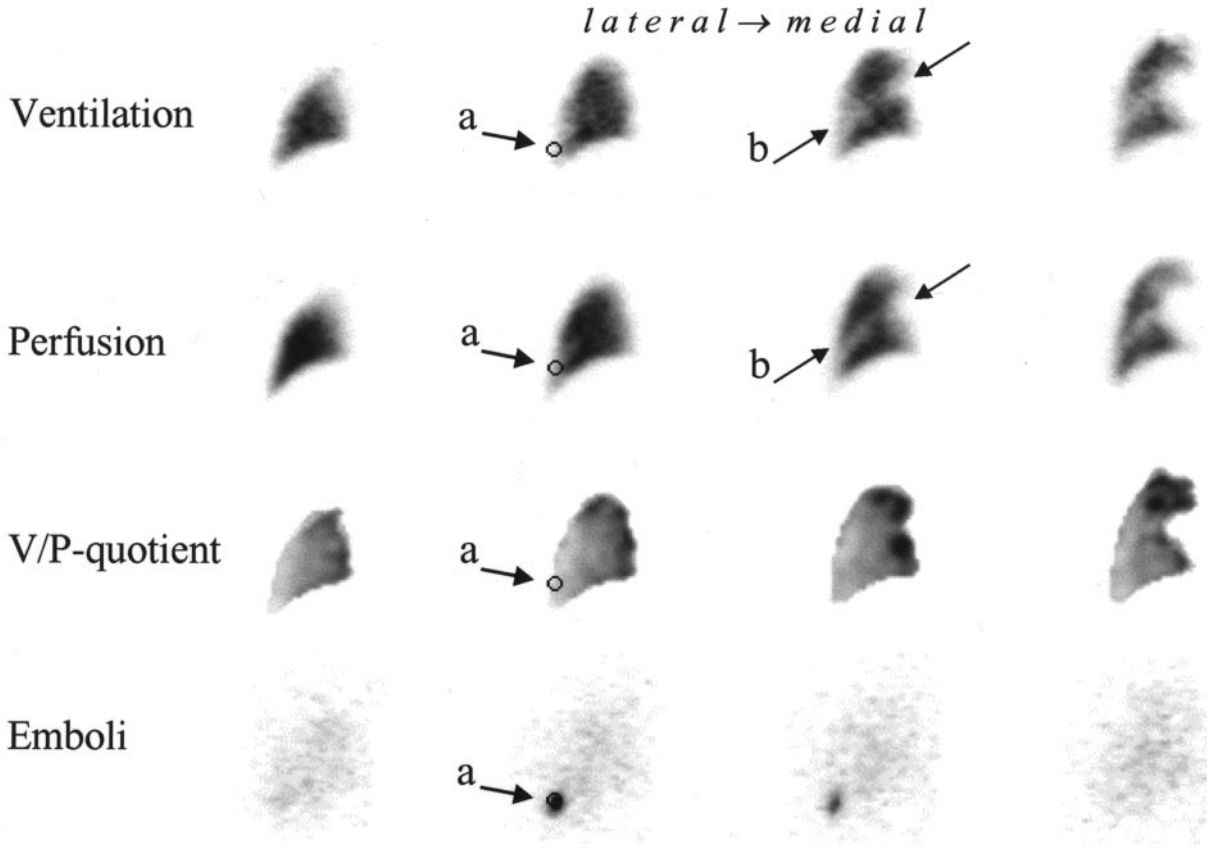

FIGURE 3. Tomography. Sagittal slices of right lung: 2 emboli lodged together in periphery of lung. Neither ventilation nor perfusion was identified distal to emboli (a), leaving V/P quotient unchanged. Anatomic configuration of main pulmonary artery causes clearly visible region with low activity on ventilation and perfusion images (b).

Our results show that the use of SPECT considerably improves the detection of very small lesions. In clinical practice, the diagnostic value of subsegmental perfusion defects is debated (*15*). Furthermore, subsegmental emboli may be of little importance for an otherwise healthy subject. However, in patients with limited cardiorespiratory reserve, small emboli may be of importance (*16*) because they may precede larger insults. In an earlier study we showed that V/P SPECT is clinically feasible with a very short acquisition time (*12*). In this study we document that SPECT is technically superior to planar scintigraphy. With respect to the above considerations, the potential improvement in clinical diagnostics of lung emboli offered by SPECT needs to be further studied.

On the basis of the recent development of CT, this method has been suggested as a first-line approach in the diagnostics of lung emboli (*17*). A higher sensitivity and better interobserver agreement of CT have been claimed (*16,17*). These arguments may be rebutted. On the basis of a recent review (*18*), Kane and Ellis (*19*) concluded that "the current available literature does not support the use of spiral CT for diagnosing pulmonary embolism" and that "the high false-negative rate prohibits its routine use as a rule out test." Other obvious limitations of CT are not always observed. A high dose of iodinated contrast material prohibits the use of CT in patients with renal failure or hypersensitivity and, to some extent, in older diabetes patients. Actual radiation exposure from CT is in the magni-

TABLE 3
Positive and Negative Findings on V/P Planar and SPECT Images of Pigs Embolized with 3-Tailed Emboli

	Planar images						SPECT images					
Reader	True-positive	False-positive	True-negative	False-negative	Sensitivity (%)	Specificity (%)	True-positive	False-positive	True-negative	False-negative	Sensitivity (%)	Specificity (%)
1	10	3	8	5	67	73	15	1	9	0	100	90
2	9	0	10	6	60	100	12	1	9	3	80	90
3	10	4	8	5	67	67	14	2	9	1	93	82

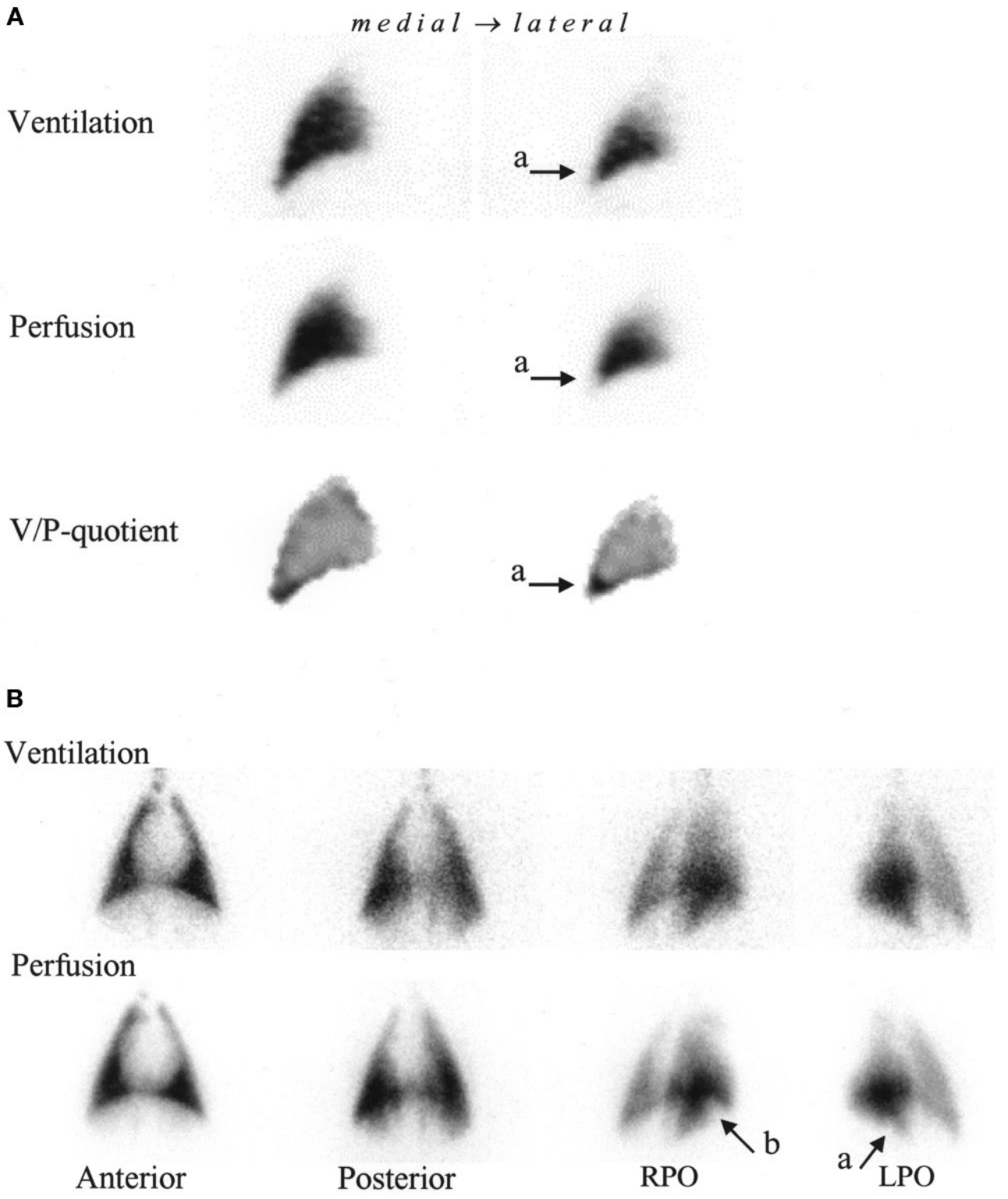

FIGURE 4. (A) Tomography. Sagittal slices of left lung: One false-positive perfusion defect was observed in nonembolized left lung (a). (B) Planar images of same pig as in A: One false-positive perfusion defect (a) and 1 true-positive perfusion defect were observed in right lung (b). RPO = right posterior oblique; LPO = left posterior oblique.

tude of 8–23 mSv (*20*) compared with 1.3 mSv from V/P SPECT with our method. Because large numbers of patients are examined and most of them do not have lung embolism, Howling and Hansell (*21*) believe that "the indiscriminate use of CT would have dire consequences in terms of radiation dose to the population as a whole."

V/P scintigraphy can be performed easily on all subjects, the radiation exposure is low, and the technique has high

sensitivity for lung emboli. However the drawbacks of scintigraphy are poor specificity and a high number of intermediary interpretations (*3*,*4*). The qualities of SPECT may minimize such problems (*9*–*12*).

We have shown in this study that V/P SPECT has similar or better sensitivity for detection of lung emboli than has been shown in another pig model for pulmonary angiography and CT (*8*). In our study, interobserver variation was smaller compared with results from angiography and CT (*22*).

V/P SPECT is a clinically feasible method that is applicable to all patients with a very short acquisition time and a low radiation exposure. Using the pig model, we showed improved sensitivity and specificity compared with that of planar imaging. Further comparison between up-to-date versions of V/P scintigraphy and spiral CT is required.

CONCLUSION

This study has verified that lung V/P SPECT is more sensitive and more accurate than planar imaging for the detection of lesions on the subsegmental level, without incurring the penalty of decreased specificity.

ACKNOWLEDGMENTS

This study was supported by the Swedish Heart and Lung Foundation and the Swedish Medical Research Council (grant 02872).

REFERENCES

1. Burkill GJ, Bell JR, Padley SP. Survey on the use of pulmonary scintigraphy, spiral CT and conventional pulmonary angiography for suspected pulmonary embolism in the British Isles. *Clin Radiol.* 1999;54:807–810.
2. ACCP Consensus Committee on Pulmonary Embolism. Opinions regarding the diagnosis and management of venous thromboembolic disease. *Chest.* 1998;113: 499–504.
3. Gottshalk A, Juni JE, Sostman HD, et al. Ventilation-perfusion scintigraphy in the PIOPED study. Part 1. Data collection and tabulation. *J Nucl Med.* 1993;34: 1109–1118.
4. Gottshalk A, Sostman HD, Coleman RE, et al. Ventilation-perfusion scintigraphy in the PIOPED study. Part 2. Evaluation of the scintigraphic criteria and interpretations. *J Nucl Med.* 1993;34:1119–1126.
5. Woodard PK. Pulmonary arteries must be seen before they can be assessed. *Radiology.* 1997;204:11–12.
6. Goodman LR, Lipchik RJ. Diagnosis of acute pulmonary embolism: time for a new approach. *Radiology.* 1996;199:25–27.
7. Remy-Jardin M, Remy J, Deschildre F, et al. Diagnosis of acute pulmonary embolism with spiral CT: comparison with pulmonary angiography and scintigraphy. *Radiology.* 1996;200:699–706.
8. Baile EM, King GG, Muller NL, at al. Spiral computed tomography is comparable to angiography for the diagnosis of pulmonary embolism. *Am J Respir Crit Care Med.* 2000;161:1010–1015.
9. Corbus HF, Seitz JP, Larson RK, et al. Diagnostic usefulness of lung SPET in pulmonary thromboembolism: an outcome study. *Nucl Med Commun.* 1997;18: 897–906.
10. Magnussen JS, Chicco P, Palmer AW, et al. Single photon emission tomography of a computerized model of pulmonary embolism. *Eur J Nucl Med.* 1999;26: 1430–1438.
11. Wenger M, Donnemiller E, Bacher-Stier C, et al. Improved pulmonary diagnosis by pixel based 3D-volume mathematics in combined inhalation/perfusion lung SPET [abstract]. *Eur J Nucl Med.* 2000;27:899.
12. Palmer J, Bitzén U, Jonson B, Bajc M. Comprehensive ventilation/perfusion SPECT. *J Nucl Med.* 2001;42:1288–1294.
13. Tägil K, Evander E, Wollmer P, Palmer J, Jonson J. Efficient lung scintigraphy. *Clin Physiol.* 2000;20:95–100.
14. Donderlinger MP, Ghysel MP, Brisbois D, et al. Relevant radiological anatomy of the pig as a training model in interventional radiology. *Eur Radiol.* 1998;8: 1254–1273.
15. Stein PD, Gottschalk A. Review of criteria appropriate for a very low probability of pulmonary embolism on ventilation-perfusion lung scans: a position paper. *Radiographics.* 2000;20:99–105.
16. Maki DD, Gefter WB, Alavi A. Recent advances in pulmonary imaging. *Chest.* 1999;116:1388–1402.
17. Mayo JR, Remy-Jardin M, Muller NL, et al. Pulmonary embolism: prospective comparison of spiral CT with ventilation/perfusion scintigraphy. *Radiology.* 1997;205:447–452.
18. Mullins MD, Becker DM, Hagspiel KD, Philbrick JT. The role of spiral volumetric computed tomography in the diagnosis of pulmonary embolism. *Arch Intern Med.* 2000;160:293–298.
19. Kane KY, Ellis MR. Is spiral (helical) computed tomography useful for diagnosing pulmonary embolism? *J Fam Pract.* 2000;49:467–468.
20. Robinson PJ. Ventilation-perfusion lung scanning and spiral computed tomography of the lungs: competing or complementary modalities? *Eur J Nucl Med.* 1996;23:1547–1553.
21. Howling SJ, Hansell DM. Spiral computed tomography for pulmonary embolism. *Hosp Med.* 2000;61:41–45.
22. Colon HO, Baile EM, King GG, et al. A method for testing the diagnostic accuracy of spiral computed tomography (CT) and pulmonary angiography for pulmonary embolism (PE) [abstract]. *Am J Respir Crit Care Med.* 2001; 163:A918.